Understanding the Stabilization of Metal Carbide Endohedral Fullerenes $M_2C_2@C_{82}$ and Related Systems

Ramón Valencia, Antonio Rodríguez-Fortea,* and Josep M. Poblet*

Departament de Química Física i Inorgànica, Universitat Rovira i Virgili, c/Marcel·lí Domingo s/n, 43007 Tarragona, Spain

Received: January 16, 2008; Revised Manuscript Received: March 7, 2008

We analyze the electronic structure of carbide endohedral metallofullerenes of the type $Sc_2C_2@C_{82}$ and study the possibility of rotation of the encapsulated Sc_2C_2 moiety in the interior of the cage. Moreover, we rationalize the higher abundance of $M_2C_2@C_{82}$ (M = Sc, Y) in which the metal−carbide cluster is encapsulated in the C_{3v}-C_{82}:**8** carbon cage with respect to other carbides of the same family on the basis of the formal transfer of four electrons from the cluster to the cage and sizeable (LUMO-3)−(LUMO-2) gap in the empty cages. This rule also applies to all those endohedral metallofullerenes in which the encapsulated cluster transfers four electrons to the carbon cage as, for example, the reduced $[M@C_{82}]^-$ systems (M = group 3 or lanthanide metal ion).

Introduction

Fullerenes with metallic atoms in their interior, i.e., the so-called endohedral metallofullerenes (EMFs), have attracted special interest during the past decade because of their exclusive properties and their potential applications in biomedicine and nanomaterials sciences.[1–3] EMFs have been found containing metal atoms, metal clusters, metal nitride clusters, and metal carbide clusters in their inner hollow space. Interestingly, the carbon cages present in EMFs are usually structural isomers of the cages found for the corresponding empty-cage fullerenes. In some cases, these cages do not fulfill the isolated pentagon rule (IPR).[4,5] A charge transfer from the encapsulated metallic cluster to the carbon framework rationalizes the existence of structural isomers that are not observed as empty-cage fullerenes.[6,7]

Since the discovery of $Sc_3N@C_{80}$ in 1999,[8] a large number of trimetallic nitride template (TNT) EMFs, $M_3N@C_{2n}$ ($2n$ = 68, 70, 78, 80, 84, 86, etc., and M = group 3 or lanthanide metal atom) have been synthesized, characterized and functionalized over the past years.[9–16] $M_3N@C_{80}$ compounds are the most abundant TNT EMFs, in which the least stable icosahedral IPR isomer of C_{80} is stabilized by the charge transferred from the TNT unit.[17] Metal−carbide EMFs have been also increasingly studied during the last years.[18–25] In these compounds, a C_2^{q-} unit ($q = 2, 3$) is encapsulated together with two or three metallic atoms (Sc, Y). Shinohara and co-workers reported in 2001 the synthesis and characterization of the first scandium−carbide metallofullerene, $Sc_2C_2@C_{84}$.[23] The formation of metal carbide EMFs with different cage sizes when performing high-resolution ion mobility measurements on $Sc_m@C_{2n}$ (m = 1–3, $2n$ = 74–90) species was also described.[26] More recently, other metal−carbide EMFs have been confirmed by ^{13}C NMR spectroscopy ($Y_2C_2@C_{82}$, $Sc_2C_2@C_{68}$),[19–21] synchrotron X-ray structural studies ($Sc_2C_2@C_{82}$, $Sc_3C_2@C_{80}$),[24,25] or even by X-ray single-crystal analysis ($Sc_2C_2@C_{82}$).[18]

SCHEME 1: Ionic Model in EMFs

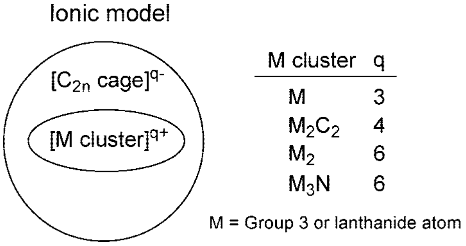

M cluster	q
M	3
M_2C_2	4
M_2	6
M_3N	6

The electronic structure of nitride EMFs can be rationalized by the following ionic model: $M_3N^{6+}@C_{2n}^{6-}$ (Scheme 1). Formally, there is a transfer of six electrons from the three highest occupied molecular orbitals (HOMOs) of the TNT unit to the three lowest unoccupied molecular orbitals (LUMOs) of the carbon cage. On the basis of this ionic electronic structure, a general rule for the stabilization of fullerene cages encapsulating TNT units has been recently established by Campanera et al. using density functional theory (DFT) methods.[27] Assuming the aforementioned six-electron transfer, the authors showed that the large HOMO−LUMO gap in nitride EMFs, which provides them with stability, can be estimated from the (LUMO-4)−(LUMO-3) gap found in the corresponding *empty* cages.[28] In particular, Campanera et al. found that the cages that had been observed to encapsulate TNT units, namely, two isomers of C_{80} (D_{5h}:**6** and I_h:**7**), one isomer of C_{78} (D_{3h}:**5**), and one non-IPR isomer of C_{68} (D_3:**6140**), feature large (LUMO-4)−(LUMO-3) gaps (larger than 1 eV in the *generalized gradient approximation* of DFT). We have recently shown that this simple rule is also valid for all the new nitride EMFs whose structures have been characterized by X-ray diffraction, i.e., one non-IPR isomer of C_{84} (C_s:**51365**), one isomer of C_{86} (D_3:**19**) and one isomer of C_{88} (D_2:**35**).[29] Moreover, we have proposed six-cage isomers as candidates for large nitride EMFs from C_{92} to C_{100} on the basis of the aforesaid simple orbital rule.[29] Recently, Popov and Dunsch have published an exhaustive study regarding the structure and the stability of nitride EMFs.[7] These authors use the stability of the empty fullerene cages in the hexaanionic state, C_{2n}^{6-}, as criterion to predict the most stable nitride EMFs. This criterion correctly predicts the cage isomers that encapsulate nitride clusters known so far. Furthermore, they have proposed

---

* Authors to whom correspondence should be addressed. E-mail: antonio.rodriguezf@urv.cat (A.R.F.); josepmaria.poblet@urv.cat (J.M.P.).

10.1021/jp800419d CCC: $40.75

SCHEME 2: Bent Geometry of Sc_2C_2 inside the C_{82} Cage

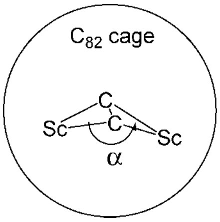

the cage isomers that should encapsulate TNTs from C_{90} to C_{98}. The proposals for large cages able to encapsulate TNTs using the simple (LUMO-4)−(LUMO-3) rule agree very well with those obtained with the more elaborated criterion of Dunsch and Popov. The only case of disagreement occurs in the C_{98} family. So, this simple orbital rule is not only able to justify which carbon cages are present in the already characterized nitride EMFs, but it also makes very reliable predictions for the encapsulation of trimetallic nitrides inside large cages.

Similarly, DFT calculations disclose that the electronic structure in carbide EMFs can be described by the ionic model $M_2C_2^{4+}@C_{2n}^{4-}$ with the transfer of four electrons from the metal carbide to the carbon cage (Scheme 1).[18] Herein, we study the electronic structure of carbide EMFs and confirm that it can be described by the ionic model $M_2C_2^{4+}@C_{2n}^{4-}$. Furthermore, we analyze the possibility of rotation of the M_2C_2 unit inside the carbon cage and rationalize the stabilization of carbide EMFs and related systems. Finally, we demonstrate that the use of a simple orbital rule derived from an ionic model of interaction, i.e., the (LUMO-3)−(LUMO-2) rule, is able to explain the larger abundance of $M_2C_2@C_{82}$ (C_{3v}:**8**) compared to other metal−carbide EMFs.

Computational Methodology

The calculations were carried out by using DFT methodology with the ADF code.[30,31] The exchange-correlation functionals of Becke[32] and Perdew[33] were used along with triple-ζ polarization basis sets to describe the valence electrons of C, Sc, and La. Frozen cores consisting of (i) the 1s shell for C; (ii) the 1s to 2p shells for Sc and (iii) the 1s to 4d shells for La, were described by means of single Slater functions. Relativistic corrections were included by means of the ZORA formalism. The geometries of all fullerene cages have been extracted from the Fullerene Structure Library created by Mitsuho Yoshida (http://www.cochem2.tutkie.tut.ac.jp/Fuller/Fuller.html). Single-point calculations were performed for all empty cages except for I_h-C_{80}:**7** and all the IPR isomers of C_{82} in their neutral and tetranionic states, which were fully optimized. Initially, all the cages have been computed as closed-shell electronic structure systems. The small number of cages whose electronic structure has not been converged as a singlet state have been recomputed as open-shell triplets. The geometries of all the EMFs computed here have been completely optimized.

Results and Discussion

1. Electronic Structure of Metal Carbide $Sc_2C_2@C_{82}$ EMFs. Our first goal is to confirm that the ionic model $(cluster)^{4+}@(cage)^{4-}$ is valid for the family $M_2C_2@C_{82}$. For that, we have optimized the geometry of six isomers of $Sc_2C_2@C_{82}$ in which the metal carbide unit Sc_2C_2 shows different orientations inside the C_{82} cage (i.e., what we call *orientational* isomers), and we have analyzed their electronic structures. We have considered that the encapsulated Sc_2C_2 unit has a bent structure (Scheme 2) and that the carbon cage is isomer C_{82}−C_{3v}:**8**, as obtained by Akasaka and Nagase from the X-ray single-crystal analysis of a carbene derivative of $Sc_2C_2@C_{82}$.[18] After the geometry optimizations, the bent geometry of the internal Sc_2C_2 is maintained.

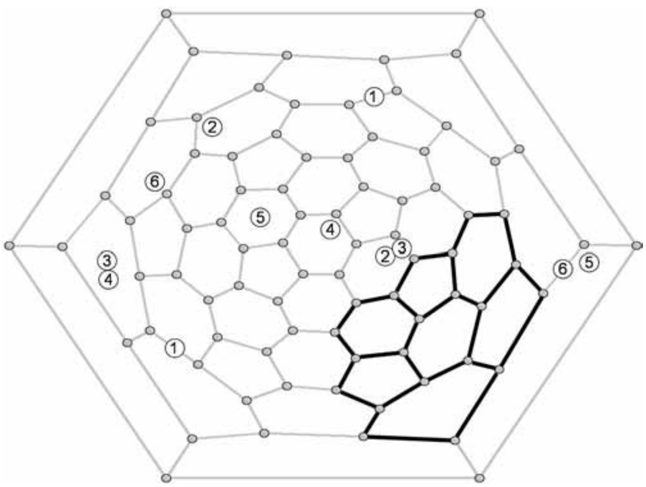

Figure 1. Schlegel diagram that represents the six orientational isomers of $Sc_2C_2@C_{82}$ studied here. The Schlegel diagram provides a 2D representation of the 3D structure of the fullerene. Since the C atoms of the Sc_2C_2 unit are placed near the centroid of the cage, we omit them for a clearer representation. The position of the Sc atoms for the different isomers is represented with numbers, i.e., the two Sc atoms of isomer **1** are represented with two 1's, the two Sc atoms of isomer **2** are represented with two 2's, and so on and so forth. The structural motif that distinguishes the C_{3v}-C_{82}:**8** from the I_h-C_{80}:**7** cage is highlighted.

TABLE 1: Most Significant Structural Parameters and Relative Energies for the Six Orientational Isomers of $Sc_2C_2@C_{82}$ (C_{3v}:8)

	Iso **1**	Iso **2**	Iso **3**	Iso **4**	Iso **5**	Iso **6**
C−C^a	1.272	1.270	1.274	1.272	1.271	1.270
Sc−C^b	2.254	2.164	2.236	2.183	2.205	2.139
	2.258	2.183	2.239	2.246	2.223	2.195
	2.296	2.444	2.264	2.324	2.282	2.410
	2.312	2.625	2.348	2.441	2.381	2.587
average	2.280	2.354	2.272	2.299	2.273	2.333
Sc−C^c	2.259	2.261	2.242	2.236	2.298	2.234
	2.272	2.295	2.307	2.310	2.301	2.281
	2.235	2.217	2.314	2.226	2.235	2.212
	2.272	2.330	2.334	2.323	2.340	2.287
α^d	124.4	115.3	147.4	124.8	144.2	116.3
ΔE^e	2.3	4.6	4.0	0.0	2.9	5.2

^{a} C−C distance in the carbide unit. ^{b} Sc−C distances within the Sc_2C_2 unit. ^{c} Sc−C distance between the Sc ions and the two nearest C atoms of the carbon cage (the first two values are for Sc1 and the other two values for Sc2). ^{d} Bent angle in the Sc_2C_2 unit. ^{e} Relative energy (in kcal mol^{-1}) with respect to the most stable isomer (**4**). Distances are in angstroms (Å) and angles are in degrees (°).

The six orientational isomers that we have studied are represented in the Schlegel diagram of Figure 1. The small energy range in which the selected isomers are found (the largest energy difference among them being 5 kcal mol^{-1}, see Table 1) indicates that some kind of rotation of the Sc_2C_2 cluster can exist in the interior of the C_{82} cage. Experimental evidence on the rotation of C_2 in Sc−carbide metallofullerenes has been reported by Shinohara et al.[34] Our result is also in good agreement with NMR experiments: (i) the 16 signals obtained in the ^{13}C NMR spectrum, consistent with the C_{3v} symmetry of

TABLE 2: Charge Transfer (in Electrons) from the Internal Cluster to the Carbon Cage in $Sc_2C_2@C_{82}$ (C_{3v}:8) and $Sc_3N@C_{80}$ (I_h:7)

	Mulliken	Hirshfeld	Voronoi	MDC-q[a]
$Sc_2C_2@C_{82}$	0.63	0.68	0.58	0.09
$Sc_3N@C_{80}$	1.28	1.10	0.94	0.92

[a] MDC-q: Multipole derived charge method.

the carbon cage, and (ii) the single line observed in the ^{45}Sc NMR spectrum, which shows that the two Sc atoms are equivalent.[18] The most significant structural features for the six isomers are collated in Table 1: the C−C and Sc−C distances within the Sc_2C_2 unit, the shortest Sc−C contacts with the cage, and the bent angle (α) of the Sc_2C_2 unit (Scheme 2). The C−C distance in the carbide is almost constant (around 1.27 Å) for the six isomers. The Sc−C distances within the Sc_2C_2 unit differ depending on the particular isomer: the four Sc−C distances are similar in isomers **1**, **3**, and **5**, whereas they are more different in isomers **2**, **4**, and **6**, making these units slightly asymmetric (two short + two long distances). The average value of the Sc−C distances for each isomer is around 2.3 Å. The distances between the Sc ions and the nearest C atoms of the cage differ somewhat from one isomer to another, being in the range between 2.21 and 2.31 Å, very similar to the Sc−C distances within the carbide. On the other hand, the shortest C···C distances between the carbide and the cage vary from 3.35 to 3.45 Å, showing that the direct interaction $C_2^{2-}\cdots C_{82}$ is small. Finally, the bent angle (α) in the carbide unit changes moderately when comparing different isomers, indicating that the Sc_2C_2 unit is quite flexible. So, the motion of the Sc_2C_2 inside the C_{82} fullerene may resemble that of a butterfly inside a cage.

From the occupation and composition of the molecular orbitals (MOs), we have verified that scandium atoms are formally Sc^{3+} ions, the C_2 unit is a carbide (C_2^{2-}), and, consequently, four electrons are transferred from the inner cluster to the carbon cage, $Sc_2C_2^{4+}@C_{82}^{4-}$. The neutral C_2 unit has the following ground-state electronic configuration: $KK(\sigma_g 2s)^2(\sigma_g{}^*2s)^2(\pi_u 2p)^4(\sigma_g 2p)^0$, with four electrons occupying the MO derived from the bonding combination of π symmetry of the 2p C atomic orbitals, i.e., $\pi_u 2p$. When the Sc_2C_2 cluster is inside the carbon cage, however, two *extra* electrons are incorporated to the C_2 unit, yielding a carbide, C_2^{2-}, now with the $\sigma_g 2p$ MO doubly occupied (Figure S1, Supporting Information). Different population analyses provide atomic charges consistent with the carbide assignment (Table S1, Supporting Information), the amount of negative charge in the C atoms of the C_2 unit being much larger than that in the C atoms of the cage. We have also compared the amount of charge transferred from the internal cluster to the carbon cage in $Sc_2C_2@C_{82}$ (formally four electrons) with that in $Sc_3N@C_{80}$ (formally six electrons) (Table 2). The four methods considered here to perform the population analyses confirm that the amount of charge transfer in carbide EMFs is much smaller than that in nitride EMFs. The value predicted for the carbide from the MDC-q method is, however, distrustfully small. The different amount of charge transfer to the carbon cage may lead to different exohedral reactivity, as noted previously for 1,3-dipolar cycloadditions in $M_3N@C_{80}$ EMFs when M = Sc is substituted by the more electropositive Y atom.[35] The study of the regioselectivity in the C_{3v}-C_{82}:**8** cage when it is externally functionalized and the comparison with the I_h-C_{80}:**7** cage will be presented in a future article.

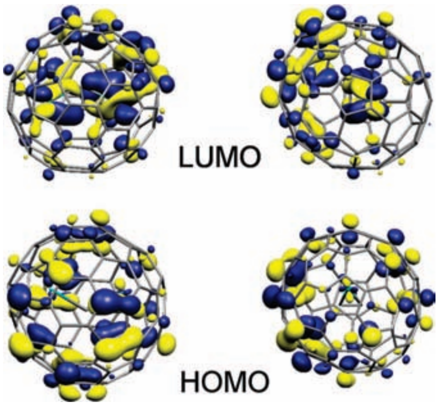

Figure 2. Two different views of the HOMO (bottom) and the LUMO (top) of the most stable orientational isomer of $M_2C_2@C_{82}$. The LUMO shows much more contribution of the inner cluster than the HOMO.

SCHEME 3: Simplified View of the Topology of the LUMO in the Internal Cluster

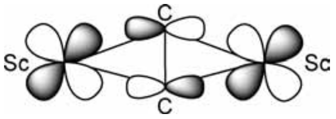

Figure 2 shows the HOMO and the LUMO of the most stable orientational isomer of $M_2C_2@C_{82}$ from the six that we have selected. The HOMOs, as well as the LUMOs, are very similar for all the orientational isomers. The HOMO shows only contribution from the carbon cage, whereas the LUMO has a significant contribution from the 3d orbitals of the Sc ions (25% cluster/75% cage, Figure 2).

Therefore, when the system is oxidized, the electron is removed exclusively from the C_{82} cage, but when the system is reduced, the incoming electron has a non-negligible probability of being found in the internal cluster. In order to verify these predictions, we have also computed the oxidized and the reduced systems, $[Sc_2C_2@C_{82}]^+$ and $[Sc_2C_2@C_{82}]^-$, respectively. From an analysis of the spin density distribution (see Supporting Information for plots of the spin density), we have confirmed that oxidation occurs in the carbon cage (spin density: 2% cluster/98% cage), whereas part of the extra electron is localized in the internal cluster when the system is reduced (spin density: 46% cluster/54% cage). A closer inspection of the topology of the LUMO reveals that the contributions of the internal cluster can be described in a simplified manner by the combination of atomic orbitals displayed in Scheme 3. There is a bonding interaction between the Sc atoms and the carbide, but an antibonding interaction exists between the two C atoms of the carbide. So, when one electron is occupying this MO (i.e., after a monoelectronic reduction), a shortening of the Sc−C distances and a lengthening of the C−C distance should occur. For reduced isomer **4**, the average of the four Sc−C distances is 2.228 Å, and the C−C distance is 1.286 Å (to be compared with 2.299 Å and 1.272 Å, respectively, for the neutral system).

2. Stabilization of C_{82} Carbide EMFs and Related Systems. The cage that encapsulates the Sc_2C_2 unit, C_{3v}-C_{82}:**8**, is the least stable isomer among the nine IPR empty-cage C_{82} fullerenes with an energy 24.6 kcal mol^{-1} higher than C_2-C_{82}:**3** (see Figure 3 and Table S2). After encapsulation and as a consequence of the electrons transferred from the internal cluster to the carbon cage, the relative stability of the isomers is altered. On the basis of the ionic model and the formal transfer of three electrons from M to the cage (Scheme 1), isomer C_{2v}:**9** has been predicted to be the cage that encapsulates the M atom (M =

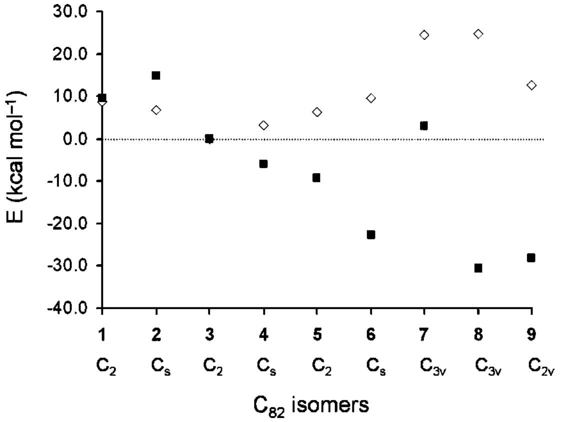

Figure 3. Energies (in kcal mol^{-1}) of C_{82} (empty diamonds) and C_{82}^{4-} isomers (filled squares) relative to C_{82}−C_2:**3** isomer. The numbering of the isomers follows the nomenclature of Fowler and Manolopoulos.[39]

TABLE 3: Relative Energies[a] and Formal Electron Transfers[b] for the Two C_{82} isomers, C_{3v}:8 and C_{2v}:9, When They Are Empty and When They Are Encapsulating a La Atom in Their Interior[c]

	C_{2v}-C_{82}:**9**	C_{3v}-C_{82}:**8**	formal transfer
empty cage	0.0	11.9	0
La@C_{82}	0.0	5.4	3
[La@C_{82}]$^-$	0.0	−2.8	4

[a] In kcal mol^{-1}. [b] Number of electrons. [c] Although different positions of the La atom inside the cage are possible, we have only computed the lowest-energy structures predicted by Kobayashi and Nagase.[36]

Group 3 or lanthanide metal atom) in the neutral M@C_{82} compounds, in good agreement with experiments.[12,36,37] These authors computed the relative stability of the trianion C_{82}^{3-} for the nine IPR structures and found that isomer C_{2v}:**9** is the most stable structure with a somewhat lower energy than isomer C_{3v}:**8**.[36] Our computations for the neutral system La@C_{82} are in agreement with the previous results, namely, the endohedral with the C_{2v}:**9** cage is more stable than that with the C_{3v}:**8** framework with an energy difference between isomers that is reduced to 5.4 kcal mol^{-1} (Table 3). For formal transfers of four electrons, as occurs for the M_2C_2@C_{82} family or the reduced [M@C_{82}]$^-$ systems, the relative stability of the different endohedrals can be predicted by computing the corresponding tetraanion C_{82}^{4-} for each isomer. The relative stability of the cages is now inverted, the three most stable isomers being C_{3v}:**8** (0.0), C_{2v}:**9** (2.4), and C_s:**6** (8.0 kcal mol^{-1}, Figure 3), in good agreement with experimental findings.[19] Moreover, for [La@C_{82}]$^-$, isomer C_{3v}:**8** is computed to be somewhat more stable than C_{2v}:**9** (Table 3). The fact that isomer C_{2v}:**9** is the cage experimentally observed in [M@C_{82}]$^-$ indicates that, after reduction of the neutral form,[37,38] kinetic products are formed. These products would have to overcome a very high barrier in order to isomerize to the most stable thermodynamic products.

3. Sc_2C_2@C_{82} (C_{3v}:8): The Most Abundant Carbide EMF Known so Far. After proving the validity of the ionic model in carbide EMFs, $Sc_2C_2^{4+}$@C_{82}^{4-}, we have computed the (LUMO-3)−(LUMO-2) gaps for the 1267 IPR structures from C_{60} to C_{100} so as to check whether other cages different from C_{82} were able to encapsulate M_2C_2 carbides. Interestingly, only the C_{3v}-C_{82}:**8** isomer shows a (LUMO-3)−(LUMO-2) gap larger than 1 eV, and no more than 2 % of the cages display a gap larger than 0.75 eV (Figure 4).

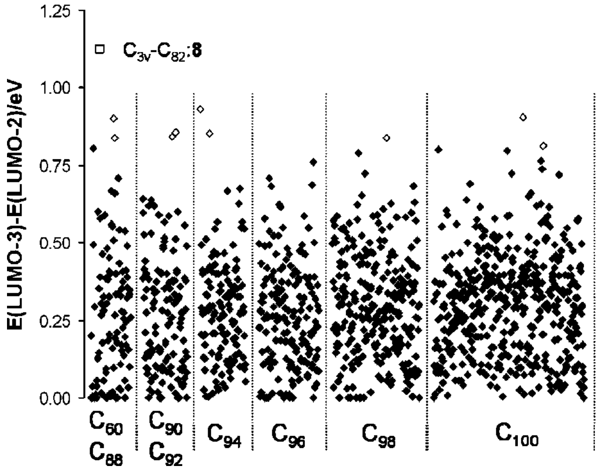

Figure 4. The (LUMO-3)−(LUMO-2) gap for each of the 1267 IPR isomers from C_{60} to C_{100}. The empty square represents the C_{3v}-C_{82}:**8** isomer, which is the cage observed in the most abundant metal−carbide EMF. Empty diamonds represent the isomers with the largest (LUMO-3)−(LUMO-2) gaps (those in Table 4), i.e., the cages with a suitable electronic structure to accept four electrons.

TABLE 4: Ten Largest Computed Values of the (LUMO-3)−(LUMO-2) Gap for the Empty Cages (in eV) from C_{60} to C_{100}

cage	isomer	(LUMO-3)−(LUMO-2) gap
C_{82}	C_{3v}-C_{82}:**8**	1.09
C_{86}	C_s-C_{86}:**8**	0.90
	C_{2v}-C_{86}:**9**	0.84
C_{92}	C_1-C_{92}:**67**	0.84
	D_3-C_{92}:**85**	0.86
C_{94}	C_3-C_{94}:**96**	0.93
	C_3-C_{94}:**110**	0.85
C_{98}	C_s-C_{98}:**151**	0.84
C_{100}	C_1-C_{100}:**17**	0.91
	C_1-C_{100}:**335**	0.81

These values, which are in general much smaller than those reported for (LUMO-4)−(LUMO-3) gaps,[29] may explain the lower stability of carbide EMFs compared to nitride endohedrals. Furthermore, isomer C_{3v}-C_{82}:**8** is the cage present in the most abundant isomer of Y_2C_2@C_{82} and the cage observed by X-ray diffraction in a carbene derivative of Sc_2C_2@C_{82}.[18,19] So, this simple orbital rule based on the charge transfer from the encapsulated metal cluster to the cage seems to work for carbide EMFs as well. No other carbon cage is predicted to form a carbide EMF as stable as M_2C_2@C_{82} (C_{3v}:**8**). Therefore, we can state that isomer C_{3v}-C_{82}:**8** is the *archetype* cage for M_2C_2 carbide EMFs, as isomer I_h-C_{80}:**7** is for nitride EMFs. Table 4 shows the 10 largest computed values of the (LUMO-3)−(LUMO-2) gap for all the empty cages from C_{60} to C_{100}. Figure 5 displays the geometry and the electronic structure of cage C_{3v}-C_{82}:**8** compared to those of I_h-C_{80}:**7**. The two geometries are related by a Stone−Wales isomerization followed by a C_2 extrusion (Scheme 4).[39] Although other mechanisms that will not be discussed here may play important roles, this two-step process may also contribute to the formation of M_2@C_{80} from M_2@C_{82} species (M = La, Ce, etc.) at high temperatures. The electronic structures of the two cages are, however, different: isomer I_h-C_{80}:**7** is stabilized by accepting six electrons, whereas isomer C_{3v}-C_{82}:**8** may be stabilized by accepting four (Figure 5).

Other M_2C_2@C_{2n} carbides exist, as for example, Sc_2C_2@C_{84}, but at lower yields compared to the most abundant Sc_2C_2@C_{82}. Although the structure of Sc_2C_2@C_{84} has not been unambiguously

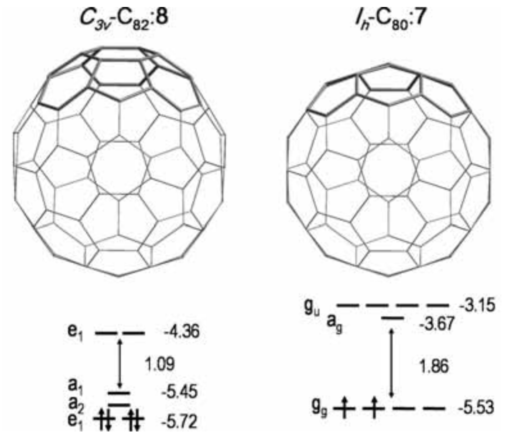

Figure 5. Comparison of geometries and electronic structures (energy, in eV, and symmetry of HOMO and LUMOs) of C_{3v}-C_{82}:**8** and I_h-C_{80}:**7**. The structural differences between the two structures are highlighted (top of the molecule).

SCHEME 4: From C_{3v}-C_{82}:8 to I_h-C_{80}:7

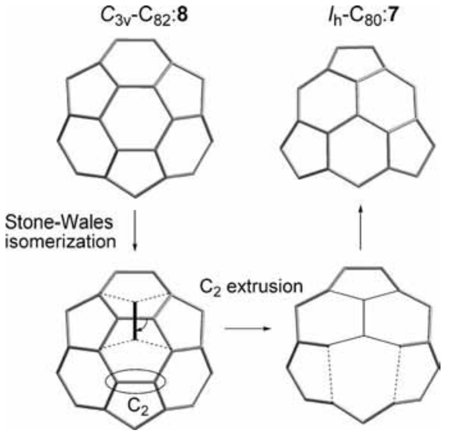

ously determined by single-crystal X-ray diffraction, the ^{13}C NMR spectrum and synchroton X-ray diffraction experiments on the powder sample indicate that the Sc_2C_2 cluster is encapsulated in the most stable empty fullerene cage (D_{2d}-C_{84}).[23] The absence of a cage isomer with a large (LUMO-3)−(LUMO-2) gap at an attainable energy in the C_{84} family leads to the encapsulation of the carbide in the most stable empty cage. On the other hand, Shinohara et al. have recently isolated and characterized the first metal carbide EMF with a non-IPR carbon cage, $Sc_2C_2@C_{68}$.[21] The non-IPR carbon cage that is supposed to encapsulate the Sc_2C_2 cluster, C_{2v}−C_{68}:**6073**, is the most stable non-IPR carbon cage with C_{2v} symmetry in the tetraanionic state, C_{68}^{4-}.[21]

Conclusions

We have confirmed that the ionic model based on the formal transfer of four electrons from the encapsulated M_2C_2 carbide to the carbon cage is valid for the $M_2C_2@C_{82}$ family. We have observed that the internal metal−carbide cluster is able to rotate inside the carbon cage. Using the aforementioned ionic model, we have understood the higher stability of $M_2C_2@C_{82}$ (C_{3v}:**8**) when compared to carbide endohedrals with other IPR C_{82} isomers. Moreover, we are able to explain the larger abundance of $M_2C_2@C_{82}$ (C_{3v}:**8**) with respect to carbide EMFs with carbon cages of different sizes, $M_2C_2@C_{2n}$ ($2n = 60, 100$). Among the 1267 IPR structures from C_{60} to C_{100}, only the C_{3v}-C_{82}:**8** isomer displays a favorable electronic structure to accept four electrons. Therefore, similarly to what occurs for the I_h-C_{80}:**7** cage in the family of nitride EMFs, we may regard the C_{3v}-C_{82}:**8** isomer as the *archetype* cage for encapsulating M_2C_2 carbides or other metal clusters, provided that four electrons are formally transferred from the cluster to the cage. Furthermore, the smaller abundance of M_2C_2 carbide EMFs with respect to nitride EMFs may be correlated to the smaller values of the (LUMO-3)−(LUMO-2) gaps of the cages that encapsulate M_2C_2 carbides as compared to the (LUMO-4)−(LUMO-3) gaps of the cages that encapsulate M_3N nitrides.

Acknowledgment. This work was supported by the Spanish Ministry of Science and Technology [Project N. CTQ2005-06909-C02-01/BQU and the Ramón y Cajal Program (A.R.F.)] and by the DURSI of the Generalitat de Catalunya (2005SGR-00104). R.V. thanks the Generalitat de Catalunya for a doctoral fellowship.

Supporting Information Available: Optimized structures (*xyz* files) of C_{3v}-C_{82}:**8**, C_{2v}-C_{82}:**9**, I_h-C_{80}:**7**, EMFs in Table 4 and the six $Sc_2C_2@C_{82}$ orientational isomers; a figure (Figure S1) showing the occupied MO of $Sc_2C_2@C_{82}$ that is empty in the neutral C_2 unit, and two figures (Figure S2a and S2b) displaying the spin-densities of $[Sc_2C_2@C_{82}]^+$ and $[Sc_2C_2@C_{82}]^-$; a table (Table S1) collating the atomic charges for different poputation analysis, and a table (Table S2) with the relative energies of neutral and tetraanionic C_{82} cages. This material is available free of charge via the Internet at http://pubs.acs.org.

References and Notes

(1) Akasaka, T.; Nagase, S. *Endofullerenes: A New Family of Carbon Clusters*; Kluwer Academic Publishers: Dordrecht, The Netherlands, 2002.

(2) Nagase, S.; Kobayashi, K.; Akasaka, T.; Wakahara, T. *Fullerenes: Chemistry, Physics and Technology*; Kadish, K., Ruoff, R. S., Eds.; John Wiley & Sons: New York, 2000; p 395.

(3) Shinohara, H. *Rep. Prog. Phys.* **2000**, *63*, 843.

(4) Beavers, C. M.; Zuo, T. M.; Duchamp, J. C.; Harich, K.; Dorn, H. C.; Olmstead, M. M.; Balch, A. L. *J. Am. Chem. Soc.* **2006**, *128*, 11352.

(5) Olmstead, M. M.; Lee, H. M.; Duchamp, J. C.; Stevenson, S.; Marciu, D.; Dorn, H. C.; Balch, A. L. *Angew. Chem., Int. Ed.* **2003**, *42*, 900.

(6) Aihara, J. *Chem. Phys. Lett.* **2001**, *343*, 465.

(7) Popov, A. A.; Dunsch, L. *J. Am. Chem. Soc.* **2007**, *129*, 11835.

(8) Stevenson, S.; Rice, G.; Glass, T.; Harich, K.; Cromer, F.; Jordan, M. R.; Craft, J.; Hadju, E.; Bible, R.; Olmstead, M. M.; Maitra, K.; Fisher, A. J.; Balch, A. L.; Dorn, H. C. *Nature* **1999**, *401*, 55.

(9) Cai, T.; Slebodnick, C.; Xu, L.; Harich, K.; Glass, T. E.; Chancellor, C.; Fettinger, J. C.; Olmstead, M. M.; Balch, A. L.; Gibson, H. W.; Dorn, H. C. *J. Am. Chem. Soc.* **2006**, *128*, 6486.

(10) Cardona, C. M.; Elliott, B.; Echegoyen, L. *J. Am. Chem. Soc.* **2006**, *128*, 6480.

(11) Cardona, C. M.; Kitaygorodskiy, A.; Echegoyen, L. *J. Am. Chem. Soc.* **2005**, *127*, 10448.

(12) Maeda, Y.; Matsunaga, Y.; Wakahara, T.; Takahashi, S.; Tsuchiya, T.; Ishitsuka, M. O.; Hasegawa, T.; Akasaka, T.; Liu, M. T. H.; Kokura, K.; Horn, E.; Yoza, K.; Kato, T.; Okubo, S.; Kobayashi, K.; Nagase, S.; Yamamoto, K. *J. Am. Chem. Soc.* **2004**, *126*, 6858.

(13) Martin, N.; Altable, M.; Filippone, S.; Martin-Domenech, A.; Echegoyen, L.; Cardona, C. M. *Angew. Chem., Int. Ed.* **2006**, *45*, 110.

(14) Olmstead, M. H.; de Bettencourt-Dias, A.; Duchamp, J. C.; Stevenson, S.; Marciu, D.; Dorn, H. C.; Balch, A. L. *Angew. Chem., Int. Ed.* **2001**, *40*, 1223.

(15) Stevenson, S.; Fowler, P. W.; Heine, T.; Duchamp, J. C.; Rice, G.; Glass, T.; Harich, K.; Hajdu, E.; Bible, R.; Dorn, H. C. *Nature* **2000**, *408*, 427.

(16) Yamada, M.; Nakahodo, T.; Wakahara, T.; Tsuchiya, T.; Maeda, Y.; Akasaka, T.; Kako, M.; Yoza, K.; Horn, E.; Mizorogi, N.; Kobayashi, K.; Nagase, S. *J. Am. Chem. Soc.* **2005**, *127*, 14570.

(17) Campanera, J. M.; Bo, C.; Olmstead, M. M.; Balch, A. L.; Poblet, J. M. *J. Phys. Chem. A* **2002**, *106*, 12356.

(18) Iiduka, Y.; Wakahara, T.; Nakajima, K.; Nakahodo, T.; Tsuchiya, T.; Maeda, Y.; Akasaka, T.; Yoza, K.; Liu, M. T. H.; Mizorogi, N.; Nagase, S. *Angew. Chem., Int. Ed.* **2007**, *46*, 5562.

(19) Inoue, T.; Tomiyama, T.; Sugai, T.; Okazaki, T.; Suematsu, T.; Fujii, N.; Utsumi, H.; Nojima, K.; Shinohara, H. *J. Phys. Chem. B* **2004**, *108*, 7573.

(20) Inoue, T.; Tomiyama, T.; Sugai, T.; Shinohara, H. *Chem. Phys. Lett.* **2003**, *382*, 226.

(21) Shi, Z. Q.; Wu, X.; Wang, C. R.; Lu, X.; Shinohara, H. *Angew. Chem., Int. Ed.* **2006**, *45*, 2107.

(22) Tan, K.; Lu, X.; Wang, C. R. *J. Phys. Chem. B* **2006**, *110*, 11098.

(23) Wang, C. R.; Kai, T.; Tomiyama, T.; Yoshida, T.; Kobayashi, Y.; Nishibori, E.; Takata, M.; Sakata, M.; Shinohara, H. *Angew. Chem., Int. Ed.* **2001**, *40*, 397.

(24) Nishibori, E.; Ishihara, M.; Takata, M.; Sakata, M.; Ito, Y.; Inoue, T.; Shinohara, H. *Chem. Phys. Lett.* **2006**, *433*, 120.

(25) Nishibori, E.; Terauchi, I.; Sakata, M.; Takata, M.; Ito, Y.; Sugai, T.; Shinohara, H. *J. Phys. Chem. B* **2006**, *110*, 19215.

(26) Sugai, T.; Inakuma, M.; Hudgins, R.; Dugourd, P.; Fye, J. L.; Jarrold, M. F.; Shinohara, H. *J. Am. Chem. Soc.* **2001**, *123*, 6427.

(27) Campanera, J. M.; Bo, C.; Poblet, J. M. *Angew. Chem., Int. Ed.* **2005**, *44*, 7230.

(28) LUMO-*n* corresponds to the *n*th lowest unoccupied molecular orbital. LUMO-1 would contain the first two electrons after a reduction, LUMO-2 the next two electrons, and so on and so forth. Hence, LUMO-3 and LUMO-4 of the empty cage would be the highest occupied and lowest unoccupied molecular orbitals, respectively, after a six-electron reduction of the cage.

(29) Valencia, R.; Rodriguez-Fortea, A.; Poblet, J. M. *Chem. Commun.* **2007**, 4161.

(30) *ADF 2004. 01*; Department of Theoretical Chemistry, Vrije Universiteit: Amsterdam, 2004.

(31) te Velde, G. T.; Bickelhaupt, F. M.; Baerends, E. J.; Guerra, C. F.; Van Gisbergen, S. J. A.; Snijders, J. G.; Ziegler, T. *J. Comput. Chem.* **2001**, *22*, 931.

(32) Becke, A. D. *Phys. Rev. A* **1988**, *38*, 3098.

(33) Perdew, J. P. *Phys. Rev. B* **1986**, *33*, 8822.

(34) Krause, M.; Hulman, M.; Kuzmany, H.; Dubay, O.; Kresse, G.; Vietze, K.; Seifert, G.; Wang, C.; Shinohara, H. *Phys. Rev. Lett.* **2004**, 93.

(35) Rodriguez-Fortea, A.; Campanera, J. M.; Cardona, C. M.; Echegoyen, L.; Poblet, J. M. *Angew. Chem., Int. Ed.* **2006**, *45*, 8176.

(36) Kobayashi, K.; Nagase, S. *Chem. Phys. Lett.* **1998**, *282*, 325.

(37) Tsuchiya, T.; Wakahara, T.; Maeda, Y.; Akasaka, T.; Waelchli, M.; Kato, T.; Okubo, H.; Mizorogi, N.; Kobayashi, K.; Nagase, S. *Angew. Chem., Int. Ed.* **2005**, *44*, 3282.

(38) Tsuchiya, T.; Sato, K.; Kurihara, H.; Wakahara, T.; Maeda, Y.; Akasaka, T.; Ohkubo, K.; Fukuzumi, S.; Kato, T.; Nagase, S. *J. Am. Chem. Soc.* **2006**, *128*, 14418.

(39) Fowler, P. W.; Manolopoulos, D. E. *An Atlas of Fullerenes*; Oxford University Press: Oxford, 1995.

JP800419D